

NEUTRON PRODUCTION AND LEAKAGE FROM MEDICAL ELECTRON ACCELERATORS *

Richard C. McCall and William P. Swanson

Stanford Linear Accelerator Center, Stanford University,
 Stanford, California 94305, U.S.A.

NEUTRON PRODUCTION

For medical accelerators operating above about 10 MeV, there is an unavoidable production of photoneutrons which add to the head leakage. The yield of photoneutrons produced by electron beams incident on thick targets has been calculated (1,2) and found to increase rapidly with primary electron energy up to approximately 25 MeV, and more slowly thereafter (Fig. 1). Dividing the neutron fluence for W (or Pb) by the photon absorbed dose (calculated by the Monte Carlo code EGS (3)) for the same conditions gives us the ratio plotted in Fig. 2. This ratio, representing the maximum achievable with practical materials, becomes nearly constant above about 25 MeV incident electron energy where its value is about 2.1×10^5 neutrons cm^{-2} rad^{-1} . Measurements that fall significantly below the curve of Fig. 2 are likely due to photon absorption in components that are not high-Z materials, or measurements made with the moveable jaws open. Points that fall significantly above probably mean there is substantial loss of electron beam elsewhere than the intended target.

Neutron spectra in the giant resonance can be adequately described by a Maxwellian distribution which involves a single parameter, the nuclear temperature T (in MeV) for the particular nucleus. The spectrum peaks at $\bar{E}_n = T$ and has an average energy of $\bar{E}_n = 2T$. The neutrons are emitted almost isotropically and values of T generally lie in the range 0.5 to 1.0 MeV for high-Z materials.

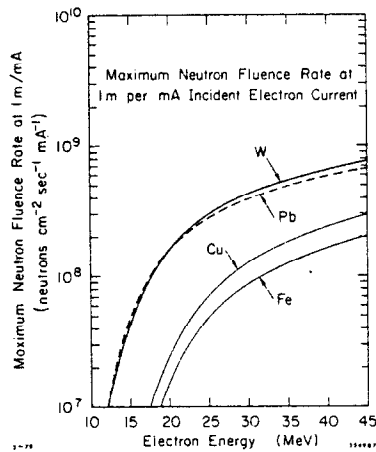


Figure 1. Maximum neutron fluence rate at 1 m.

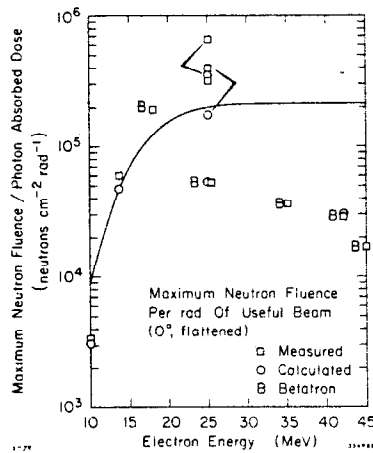


Figure 2. Neutron fluence per treatment rad (0° , flattened).

* This work was supported by the Department of Energy under Contract Number DE-AC03-76SF00515.

DEGRADATION OF NEUTRON ENERGY IN THE TREATMENT HEAD

The typical medical accelerator has massive shielding around the target to provide photon shielding and produce a collimated beam of x-rays. The photon shielding is of some heavy metal such as W or Pb, with some Fe and Cu present. The significant neutron energy loss mechanisms in the heavy elements are inelastic scattering and (n,2n) reactions. Because these cross sections together amount to 1-2 b in W and Pb, the typical neutron undergoes several collisions within the shielding. In addition, a large amount of elastic scattering takes place (4-5 b). This increases the effective path length in the shielding, thereby offering greater opportunity for inelastic reactions. Although the energy degradation is significant, the attenuation of neutron fluence is small because the capture cross sections of W and Pb are small down to thermal energies. Fig. 3 shows the integral photoneutron spectra for 15-MeV electrons on W and for ^{252}Cf fission neutrons; these are quite similar. On the same figure, we show the neutron spectrum from 15-MeV electrons on W after the neutrons have penetrated 10 cm of W. Also shown is the further degradation due to reflection in the concrete room in which medical accelerators are usually placed. Concrete-scattered neutrons add to the neutron fluence but their contribution to the patient's dose is much smaller, because of the lower energy spectrum. The average energy of the room-energy component is about $\frac{1}{4}$ of that of the direct component.

NEUTRON SOURCES IN A MEDICAL ACCELERATOR

Most medical linacs provide fields up to about $35 \times 35 \text{ cm}^2$ at 100 cm from the target. The main collimator covers all forward directions beyond the extremes, with a half-angle of about 14 degrees. If the target, flattener, jaws and main collimator are of the same material, it would be W or Pb which have nearly equal neutron yields (1). Only photons above about 8 MeV are effective in producing neutrons.

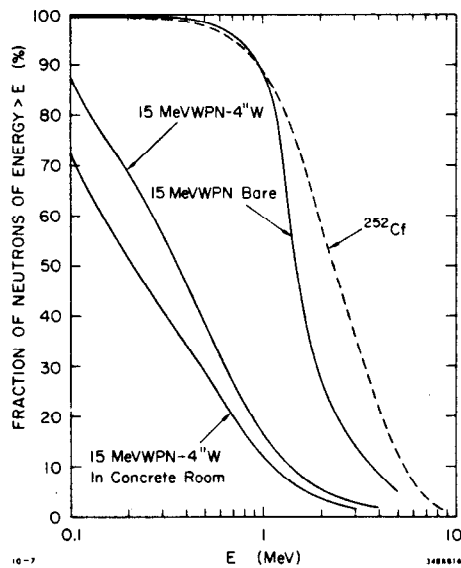


Figure 3. Neutron integral spectra, modified by shielding.

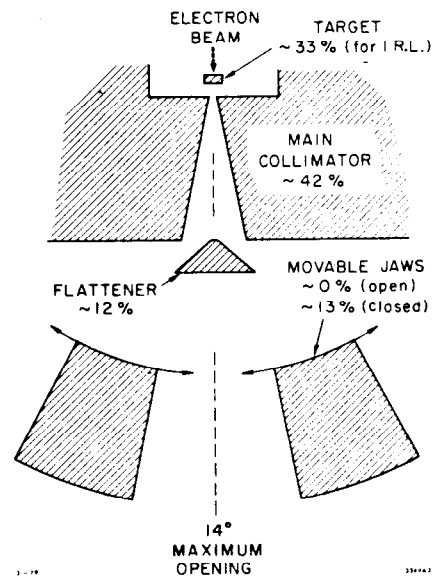


Figure 4. Neutron-producing components (not to scale).

These are mostly forward-directed and are absorbed in the main collimator or pass through and strike the flattener or the jaws. Using the Monte Carlo program EGS (3), we have calculated the angular distribution of photons of energy above 8 MeV (4). Using this angular distribution and the neutron yield as a function of material thickness (1) we have calculated the neutron yield from treatment head components. This is done for the choices of materials summarized in Table 1.

TABLE 1. Summary of Neutron Source Calculations (25 MeV Electrons).

Material and Percentage of Neutrons			Fraction of Infinite W Yield	Neutrons per rad
Target	Flattener	Main Collimator		
W 38%	W 14%	W 48%	86.5%	2.2×10^{10}
W 43%	Fe 2%	W 55%	64%	1.6×10^{10}
Cu 9.2%	W 30%	W 60.5%	84%	2.1×10^{10}
Cu 12.5%	Fe 5.7%	W 82%	64%	1.6×10^{10}

The yields for an all-W design are also shown as percentages of the maximum possible in Fig. 4. Note that while the total neutron yield is not very different for the choices of materials given in Table 1, the fraction from different components varies. Similar calculations and measurements of total fast-neutron source strengths (5) for several accelerator models (Table 2) indicate that the overall head leakage can be calculated with an accuracy no worse than about $\pm 50\%$.

TABLE 2. Calculated and Measured Neutron Yield per Photon rad.

Accelerator	Energy (MeV)	Relative Neutron Yield (n/rad)	
		Calculated	Measured
ATC 25 MeV Betatron	25	6.8×10^9	6.9×10^9
Siemens 42 MeV Betatron	42	3.8×10^9	3.7×10^9
Varian Clinac 35 (Old)	25	4.3×10^{10}	8.1×10^{10}
Varian Clinac 35 (New)	25	2.2×10^{10}	6.2×10^{10}
Varian Clinac 18	10	3.9×10^8	4.2×10^8
Siemens Mevatron XX	15	5.8×10^9	7.6×10^9

LEAKAGE NEUTRON DEPTH-DOSE CURVES

Because the leakage neutrons are considerable degraded in energy, one would expect them to be attenuated quite rapidly in tissue. We have calculated this depth-dose distribution using the computer code MORSE (6), in which the source spectrum used was that of either a 14-MeV or 25-MeV (incident electron energy) photoneutron spectrum

surrounded by 10 cm of W. The phantom was a 1-m \times 30-cm (diam) H₂O cylinder, centered at 1 m from the point source and oriented perpendicularly to the beam direction. Fig. 5 shows the rapid falloff of absorbed dose of these two spectra.

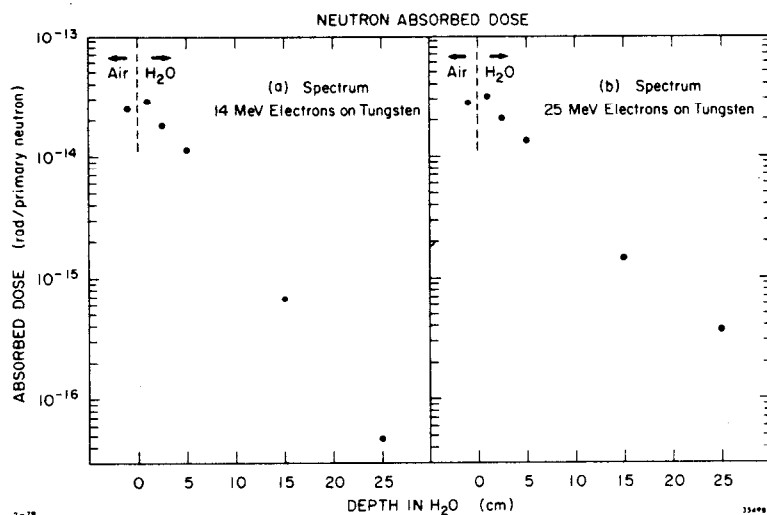


Figure 5. Depth-dose distributions in H₂O for neutron spectra from therapy targets, modified by 10 cm of W.

REFERENCES

1. Swanson, W. P. (1979): Health Phys. 37, 347.
2. Swanson, W. P. (1978): Health Phys. 35, 353.
3. Ford, R. L. and Nelson, W. R. (1978): The EGS Code System: Computer Programs for the Monte-Carlo Simulation of Electromagnetic Showers (Version 3), SLAC Report No. SLAC-210.
4. McCall, R. C. and Swanson, W. P. (1979): Proceedings of the NBS-BRH Conference on Neutrons from Electron Medical Accelerators, held at Gaithersburg, MD, April 9-10, 1979, NBS Special Publication No. 554, p. 75; and SLAC Report No. SLAC-PUB-2292.
5. McCall, R. C., Jenkins, T. M. and Shore, R. A. (1978): IEEE Trans. Nucl. Sci. NS-26, No. 1, 1593; and SLAC Report No. SLAC-PUB-2214.
6. Straker, E. A., Stevens, P. N., Irving, C. C. and Cain, V. R. (1976): The MORSE Code - A Multi-Group Neutron and Gamma Ray Monte-Carlo Transport Code, Report No. ORNL-4583; Also see Radiation Shielding Information Center, Report No. CCC-203 (1976).